Structure of the Membrane Protein FhaC: A Member of the Omp85-TpsB Transporter Superfamily

Bernard Clantin, *et al.*

Science **317**, 957 (2007);
DOI: 10.1126/science.1143860

Science (print ISSN 0036-8075; online ISSN 1095-9203) is published weekly, except the last week in December, by the American Association for the Advancement of Science, 1200 New York Avenue NW, Washington, DC 20005.

References and Notes

1. G. Stange, S. Stowe, *Microsc. Res. Tech.* **47**, 416 (1999).
2. S. Lahiri, R. E. Forster 2nd, *Int. J. Biochem. Cell Biol.* **35**, 1413 (2003).
3. M. T. Gillies, *Bull. Entomol. Res.* **70**, 525 (1980).
4. G. S. Suh *et al.*, *Nature* **431**, 854 (2004).
5. C. Thom, P. G. Guerenstein, W. L. Mechaber, J. G. Hildebrand, *J. Chem. Ecol.* **30**, 1285 (2004).
6. W. D. Jones, P. Cayirlioglu, I. G. Kadow, L. B. Vosshall, *Nature* **445**, 86 (2007).
7. D. Shusterman, P. C. Avila, *Chem. Senses* **28**, 595 (2003).
8. E. L. Coates, *Respir. Physiol.* **129**, 219 (2001).
9. M. Kimoto *et al.*, *J. Histochem. Cytochem.* **52**, 1057 (2004).
10. S. L. Youngentob, D. E. Hornung, M. M. Mozell, *Physiol. Behav.* **49**, 21 (1991).
11. K. E. Ferris, R. D. Clark, E. L. Coates, *Chem. Senses* **32**, 263 (2007).
12. H. J. Fulle *et al.*, *Proc. Natl. Acad. Sci. U.S.A.* **92**, 3571 (1995).
13. D. M. Juilfs *et al.*, *Proc. Natl. Acad. Sci. U.S.A.* **94**, 3388 (1997).
14. M. R. Meyer, A. Angele, E. Kremmer, U. B. Kaupp, F. Muller, *Proc. Natl. Acad. Sci. U.S.A.* **97**, 10595 (2000).
15. K. Shinoda, T. Ohtsuki, M. Nagano, T. Okumura, *Brain Res.* **618**, 160 (1993).
16. M. H. Teicher, W. B. Stewart, J. S. Kauer, G. M. Shepherd, *Brain Res.* **194**, 530 (1980).
17. W. Lin, J. Arellano, B. Slotnick, D. Restrepo, *J. Neurosci.* **24**, 3703 (2004).
18. Materials and methods are available as supporting material on *Science* Online.
19. R. G. Khalifah, *J. Biol. Chem.* **246**, 2561 (1971).
20. P. Pan *et al.*, *J. Physiol.* **571**, 319 (2006).
21. M. Ma, G. M. Shepherd, *Proc. Natl. Acad. Sci. U.S.A.* **97**, 12869 (2000).
22. H. Harned, R. J. Davis, *J. Am. Chem. Soc.* **65**, 2030 (1943).
23. T. Y. Chen *et al.*, *Nature* **362**, 764 (1993).
24. A. C. Clevenger, D. Restrepo, *Chem. Senses* **31**, 9 (2006).
25. K. McBride, B. Slotnick, F. L. Margolis, *Chem. Senses* **28**, 659 (2003).
26. S. E. Lewis, R. P. Erickson, L. B. Barnett, P. J. Venta, R. E. Tashian, *Proc. Natl. Acad. Sci. U.S.A.* **85**, 1962 (1988).
27. L. J. Brunet, G. H. Gold, J. Ngai, *Neuron* **17**, 681 (1996).
28. P. N. Pearson, M. R. Palmer, *Nature* **406**, 695 (2000).
29. P. M. Cox, R. A. Betts, C. D. Jones, S. A. Spall, I. J. Totterdell, *Nature* **408**, 184 (2000).

30. We dedicate this paper to the memory of L. C. Katz. We thank H. Zhao for *CNGA2*-knockout mice; J. A. Beavo for antibodies against PDE2A; C. Zhan, Y. Lu, and M. Kubota for technical assistance; M. Ma for technical advice; and A. Person, P. Sterling, and R. Roberts for comments on the manuscript. M.L. is supported by the China Ministry of Science and Technology, a Natural Science Foundation of China Young-Investigator Grant, and a Human Frontier Science Program grant jointly to H.M. and M.L. Support from NIH grants went to H.M., A.W., and P.M. Questions about GCD-ITG mice should be addressed to P.M. (peter@rockefeller.edu).

Supporting Online Material

www.sciencemag.org/cgi/content/full/317/5840/953/DC1
Materials and Methods
Figs. S1 to S13
References

25 April 2007; accepted 12 July 2007
10.1126/science.1144233

Structure of the Membrane Protein FhaC: A Member of the Omp85-TpsB Transporter Superfamily

Bernard Clantin,[1,2,3] Anne-Sophie Delattre,[2,3,4] Prakash Rucktooa,[1,2,3] Nathalie Saint,[5,6] Albano C. Méli,[5,6] Camille Locht,[2,3,4] Françoise Jacob-Dubuisson,[2,3,4]* Vincent Villeret[1,2,3]*

In Gram-negative bacteria and eukaryotic organelles, β-barrel proteins of the outer membrane protein 85–two-partner secretion B (Omp85-TpsB) superfamily are essential components of protein transport machineries. The TpsB transporter FhaC mediates the secretion of *Bordetella pertussis* filamentous hemagglutinin (FHA). We report the 3.15 Å crystal structure of FhaC. The transporter comprises a 16-stranded β barrel that is occluded by an N-terminal α helix and an extracellular loop and a periplasmic module composed of two aligned polypeptide-transport–associated (POTRA) domains. Functional data reveal that FHA binds to the POTRA 1 domain via its N-terminal domain and likely translocates the adhesin-repeated motifs in an extended hairpin conformation, with folding occurring at the cell surface. General features of the mechanism obtained here are likely to apply throughout the superfamily.

Targeting of proteins to their dedicated subcellular compartments is essential for cell function and organelle biogenesis. Translocation of proteins across or insertion into membranes is mediated by protein machineries, some of which have been conserved throughout evolution, such as the transporters of the Omp85-TpsB superfamily. TpsB transporters are components of two-partner secretion (TPS) systems in Gram-negative bacteria. They secrete large, mostly β-helical proteins called TpsA proteins that generally serve as virulence factors (*1*, *2*). TpsB transporters function without accessory factors. The superfamily also includes the Toc75, Sam50-Tob55, and Omp85-YaeT homologs, which are the cores of large hetero-oligomeric complexes involved in protein transport across, and insertion of β-barrel proteins into, the outer membranes of chloroplasts, mitochondria, and Gram-negative bacteria, respectively (*3*–*9*).

Omp85-TpsB transporters have been predicted to comprise a conserved C-terminal transmembrane β barrel and a soluble N-terminal region harboring one to five putative polypeptide-transport-associated (POTRA) domains, which are hypothesized to mediate protein-protein interactions (*10*–*12*). The transporters also harbor conserved C-proximal signature motifs of unknown function in their pore-forming regions (*13*). In spite of their implication in critical physiological processes such as membrane biogenesis and secretion of virulence proteins, the molecular mechanisms of protein translocation or insertion into membranes by those transporters remain poorly understood. To address these issues, we determined the crystal structure of the TpsB prototype FhaC that mediates the translocation to the bacterial surface of filamentous hemagglutinin (FHA), the major adhesin of the whooping cough agent *Bordetella pertussis*.

FhaC was crystallized in space group $C222_1$, and the crystals contained one molecule in the asymmetric unit. The structure was solved by the single-wavelength anomalous diffusion (SAD) method (*14*) and is reported to a resolution of 3.15 Å (table S1 and fig. S1). The protein is a monomer and comprises a 35 Å high β barrel composed of 16 antiparallel β strands (B1 to B16) (Fig. 1A and fig. S2) with a shear number of 20. The β barrel corresponds to the C-terminal moiety of the protein and encompasses residues 209 to 554. The periplasmic and extracellular sides of the barrel are characterized by short turns and longer loops (L1 to L8), respectively, in general agreement with a prior topology model (*15*). The N terminus of the protein is located in the extracellular milieu and folds into a 20-residue-long α helix (H1) that goes right through the transmembrane β barrel (Fig. 1, A and B). The C terminus of helix H1 emerges into the periplasm and is connected to a periplasmic module via a 30–amino acids linker that has no well-defined electron density in the crystal structure. This periplasmic module of 150 residues precedes the β barrel, a feature that had not been predicted earlier (*15*).

The interior of the β barrel is partly hydrophilic, with 17 charged residues pointing inward. Helix H1 is also charged with six Lys and/or Arg and six Asp and/or Glu residues. The charged residues are not uniformly distributed inside the barrel but form three clusters (fig. S3). Cluster 1 runs from the periplasm to the bacterial surface and comprises residues Arg^{280} and Asp^{282} (B5), Lys^{313} (B6), Lys^{333} and Arg^{335} (B7), Asp^{355} (B8), and

[1]UMR8161 CNRS, Institut de Biologie de Lille, Université de Lille 1, Université de Lille 2, 1 rue du Prof. Calmette, F-59021 Lille cedex, France. [2]Institut Pasteur de Lille, Lille, 1 rue du Prof. Calmette, F-59019 Lille cedex, France. [3]IFR142, 59019 Lille, France. [4]INSERM, U629, 59019 Lille, France. [5]INSERM, U554, 34090 Montpellier, France. [6]UMR5048 CNRS, Université de Montpellier 1, Université de Montpellier 2, Montpellier, France.

*To whom correspondence should be addressed. E-mail: francoise.jacob@ibl.fr (F.J.-D.); vincent.villeret@ibl.fr (V.V.)

Arg^{402} (B10) (fig. S3A). They are complemented by residues from H1 (Arg^{13}, Asp^{15}, Asp^{16}, and Arg^{19}). Cluster 2 comprises residues Asp^{218} (B1), Lys^{231} (B2), Arg^{255} (B3), and Glu^{265} (B4) and is located close to the extracellular side. Lastly, cluster 3 comprises residues—Lys^{481} (loop B12-B13), Arg^{516} and Asp^{518} (B14), and Arg^{523} (B15)—close to the periplasmic side of the β barrel (fig. S3B). The large extracellular loop L6 (residues 431 to 469) is folded as a hairpin in the barrel interior, with its tip reaching the periplasm (Fig. 1B). This loop, which is not rigidly bound to the β barrel, covers the inner face of the barrel comprising strands B11 to B16 (fig. S3C). Loop L6 is not well defined in the electron density map and was therefore built as a polyalanine chain. The average temperature factor for Cα in loop L6 is 65 $Å^2$, compared to an overall Cα temperature factor of 38 $Å^2$ in FhaC.

Analyses of the pore dimension (fig. S4A) indicate that the channel in FhaC is too narrow to accommodate the transiting FHA polypeptide because the constricted channel running from the periplasm to the surface between H1 and L6 is only ~3 Å. FhaC forms ion-permeable channels in artificial membranes with conductance values around 1.2 nS in 1 M KCl (*16*). Assuming that the protein forms a perfect cylinder, the pore diameter calculated (*17*) from the measured conductance would be 8.2 Å. However, conductance is not simply related to the size of the channel opening but also to the distribution and environment of the charges inside the channel. Thus, the observed conductance most likely reflects large conformational changes in FhaC in the electrophysiological experiments, possibly with H1 and/or L6 moving out of the pore.

The periplasmic module consists of two globular domains. Both are composed of 75 residues (from 59 to 134 and 135 to 208, respectively) and are organized around a three-stranded β sheet and one α helix (designated hereafter as a POTRA helix). They share the same strand-helix-strand-strand topology. Domain 1 (POTRA 1) corresponds in sequence to the in silico–predicted POTRA domain of the Omp85-TpsB superfamily (*11*). Domain 2 was not previously predicted to also adopt this architecture. Between the first strand and the POTRA helix, the POTRA domains also comprise either an additional turn of α helix and a loop (POTRA 1) or a 10-residue-long additional α helix (POTRA 2) (Fig. 1A and fig. S2). The relative orientation of the POTRA domains was assessed by comparing the angles formed between the axes of helices H2 and H4 with the central axis of the FhaC β barrel. The POTRA 1 and POTRA 2 angles are 148° and 111°, respectively. The two POTRA domains interact with each other via a few hydrogen bonds between loops H2-β2 and H3-H4. POTRA helices H2 and H4, together with strands β5 and β6 (POTRA 2), constitute the surface of the periplasmic module, which is oriented toward the barrel (fig. S5) and close to the translocation pore.

Although well conserved in structure (*18*), the POTRA domains are only 14% identical in sequence. Residues forming the POTRA signature (*11*) either are involved in the hydrophobic core defined by the POTRA helix and the three-stranded β sheet or correspond to glycine residues in loops, such as Gly^{69} and Gly^{109} in loops β1-H2 and H2-β2 for POTRA 1 and Gly^{143} and Gly^{182} in loops β4-H3 and H4-β5 for POTRA 2, respectively (Fig. 2A). Another residue of the POTRA signature, Gly^{134}, is located at the POTRA domains junction. The contribution of these signature residues is essentially structural, and therefore the solvent-accessible surfaces of the POTRA domains are mostly made up of nonconserved, specific residues.

Besides representing the TpsB family, the FhaC structure is also representative of more distantly related transporters of the superfamily, which all share a common architecture consisting of a variable number of POTRA domains in tandem followed by a C-terminal, ≈30-kD β-barrel domain (*10*). In silico analyses of this superfamily have also pinpointed conserved motifs within the β barrel, called motifs 3 and 4 (*13*). In FhaC, motif 3 (amino acids 432 to 474) (Fig. 1) comprises loop L6 and the first half of strand B12. The conserved tetrad VRGY (*19*) (residues 449 to 452) is located at the extremity of the β hairpin in loop L6 and reaches the periplasm. Motif 4 (residues 508 to 536) corresponds to strands B14 and B15, thus comprising residues from the inner and outer faces of the barrel. Residues Met^{508}, Arg^{516}, and Asp^{518} (B14) and Arg^{523}, Ser^{525}, Thr^{527}, and Ser^{529} (B15) are located in the vicinity of loop L6, on the inner face of the β barrel. Motif 4 also comprises residues from the uncharged inner face of the β barrel, along which loop L6 is positioned (fig. S3C).

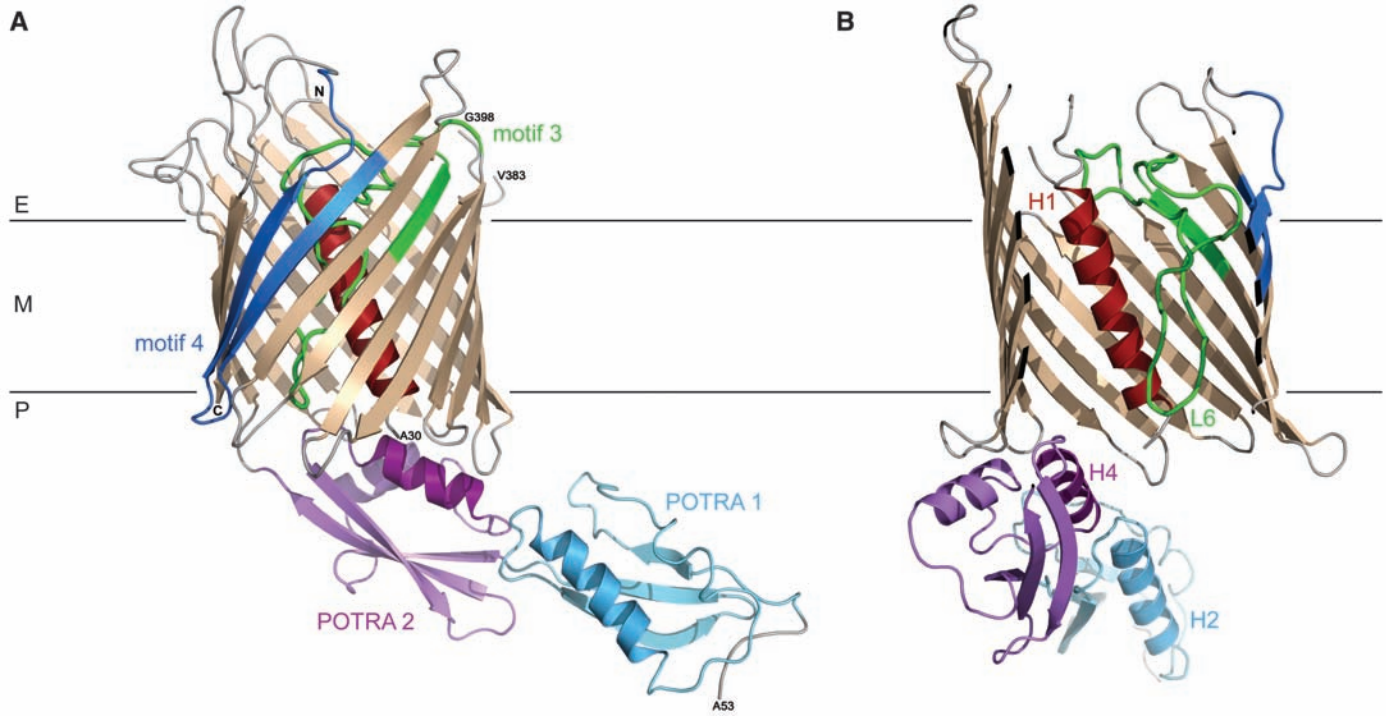

Fig. 1. Crystal structure of FhaC. (**A**) Ribbon representation of FhaC viewed from the membrane plane. Putative position of the membrane (M) boundary is indicated with horizontal lines, with the extracellular side (E) at the top and the periplasm (P) at the bottom. The α helix H1 is colored red, POTRA 1 light blue, POTRA 2 purple, motif 3 green, and motif 4 blue. (**B**) Cutaway view of FhaC from the membrane plane, rotated about 90° relative to A. The α helix H1, POTRA helices H2 and H4, and the loop L6 are indicated. The images were created with PyMOL (*30*).

In light of the crystal structure, functional aspects of FHA translocation by FhaC have been probed by mutation and deletion studies. FHA secretion has previously been shown to not be affected by removing helix H1 (*15*, *16*), ruling out an essential contribution of H1 in facilitating secretion. FhaC lacking H1 forms channels of similar conductance to that of the wild-type protein in planar lipid bilayer experiments (*16*). Removing H1 would create a ~8 Å large pore (fig. S4B) in FhaC, a size compatible with the conductances observed for both the native and the truncated proteins. These data are in agreement with a model in which H1, found inside the pore in the crystal structure, would be located outside the pore in the electrophysiological experiments. This is similar to previous observations on the crystal structure and electrophysiological data of the translocator domain of the NalP autotransporter (*20*, *21*). Also similar to NalP, the removal of H1 from FhaC enlarges the channel in vivo, as assessed by increased sensitivity to antibiotics (table S2).

In contrast to H1, the deletion of L6 performed in this work abolished secretion, demonstrating its key role in the secretion mechanism (Fig. 3A). This deletion also strongly affected the channel properties of FhaC and decreased the observed conductance to 0.4 to 0.6 nS (Fig. 3). Although removing L6 is predicted to create a 8 Å large channel in FhaC (fig. S4C), the reduction of ion conductance suggests that it affects the conformational stability of the protein and causes important charge rearrangements inside the channel. Crystal structures of OmpF in which the constriction loop L3 has been altered or partially deleted have revealed an increase of the channel size by about 50%, although the ion conductances of these mutants were drastically reduced (*22*–*24*). Evidence for the formation of larger channels by FhaC lacking L6 was obtained from antibiotic sensitivity experiments (table S2), consistent with a role for L6 in plugging the channel. A protease-specific cleavage site inserted after Ser^{462} of FhaC was previously shown to be accessible from the bacterial surface only when FHA is coproduced with FhaC (*15*), indicating conformational changes of L6 during secretion.

The deletion of either POTRA domain, performed here, also abolishes secretion, although FhaC still forms channels in lipid bilayers (Fig. 3, E and F). Therefore, the POTRA domains are strictly required for the secretion process but not for pore formation. The precise orientation of the two POTRA domains is also required, because the insertion of a glycine-serine motif immediately after the conserved Gly^{134} residue of the POTRA sequence signature at the junction of the POTRA domains strongly affects secretion, as shown previously (*15*).

The POTRA domains are involved in FHA recognition, which is likely related to their function in secretion (*25*). Previous work has shown that they recognize a nonnative state of FHA, presumably corresponding to its extended periplasmic conformation in the course of secretion (*25*). In order to identify regions of the POTRA domains involved in these interactions, we interpreted a previously reported insertional analysis in the context of the structure, looking at the effect of insertions in the solvent-exposed regions of the POTRA domains, and we complemented this data with site-directed mutagenesis (Fig. 2B). Insertions of two-residue motifs after positions 72, 73, 79, 88, 93, and 125 (in POTRA 1) and 150, 193, and 206 (in POTRA 2) were shown previously to not affect FHA secretion (*15*), ruling out a major role for these regions in the specific recognition of FHA and in the secretion process. The targeted regions, loop β1-H2 (72-93), loop β2-β3 (125), and helix H3 (150), are located on the faces of the POTRA domains pointing away from the β barrel pore. Thus, the structure rationalizes why they do not affect secretion (Fig. 2B). Insertions in loop β5-β6 (193) and in strand β6 (206) (*15*) are oriented toward the β barrel interior, but because they do not affect secretion they presumably are not major FHA recognition determinants. Therefore, specific interactions of the POTRA domains with FHA likely involve their remaining solvent-exposed surfaces, including helix H2, helix H4, and/or strand β5. Residues located on the exposed faces of these secondary structures that might form hydrogen bonds with FHA, in H2 [K99, Y106, D107, or R108 (*19*)], H4 (D173 or Y177), and strand β5 (T185 or N187), were thus replaced by alanines. Both sin-

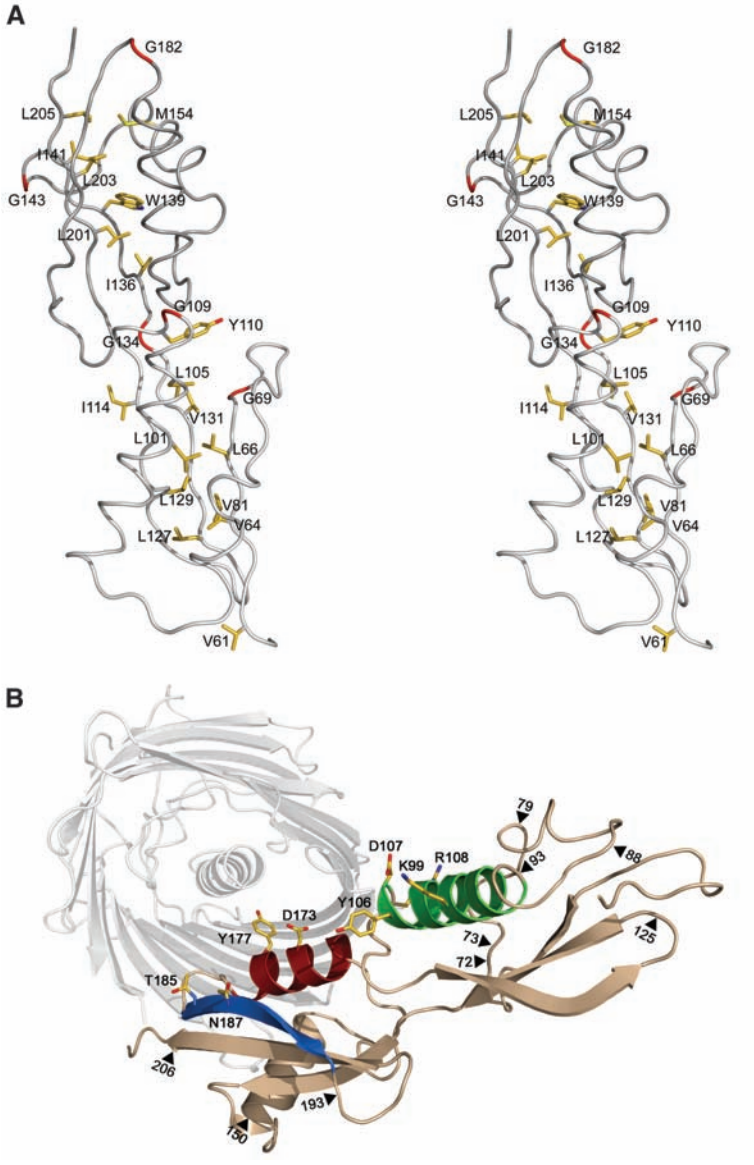

Fig. 2. (**A**) Cα stereoview of the two POTRA domains. POTRA signature residues (*11*) involved in the hydrophobic core are shown in stick representation, whereas the conserved glycines are colored red. V61 and I114 do not belong to the hydrophobic core of POTRA 1. (**B**) Ribbon representation of FhaC viewed from the periplasm. Insertion positions of the two-residue motifs are indicated by black triangles. Side chains of residues analyzed by site-directed mutagenesis are shown with a stick representation. H2, H4, and β5 are colored green, red, and blue, respectively.

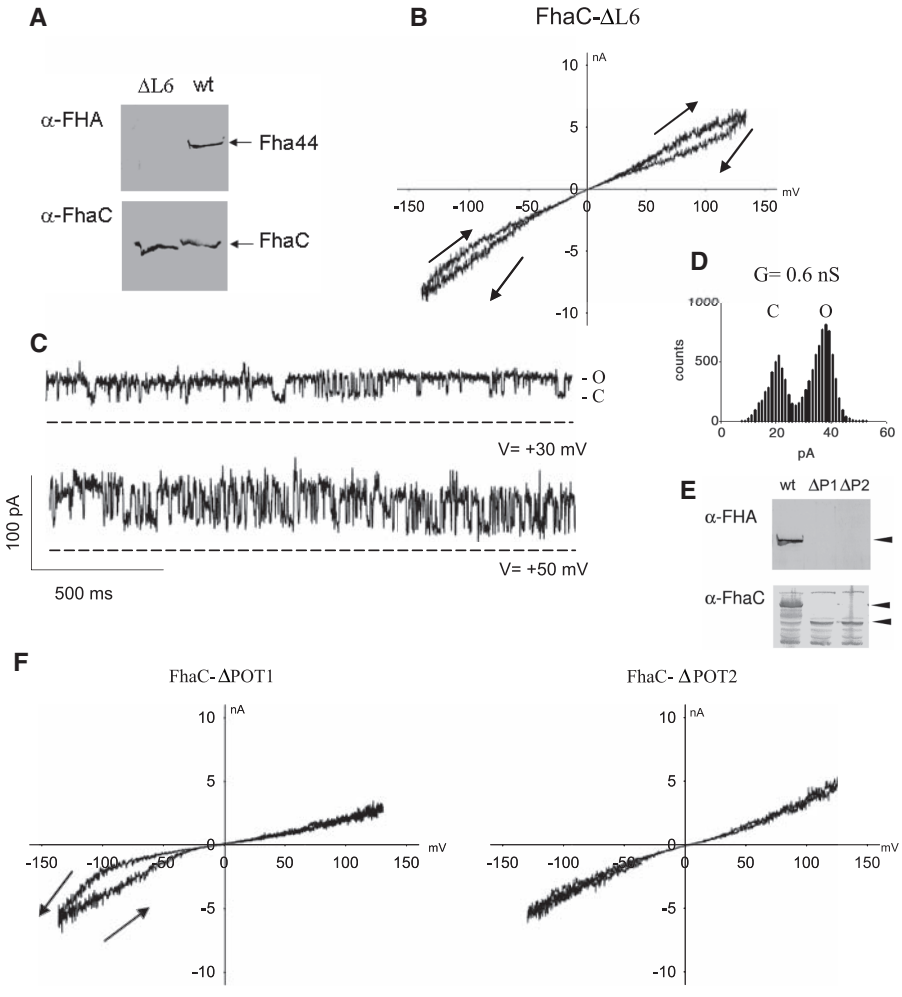

Fig. 3. (**A** to **D**) Behavior of FhaC-ΔL6. (A) Secretion of Fha44, an FHA derivative used as a model FhaC substrate in *Escherichia coli*, by UT5600 (pFJD12, pFc33) (right lanes) and UT5600 (pFJD12, pAS-FcΔL6) (left lanes). Fha44 (top) and FhaC (bottom) were detected with appropriate antibodies by immunoblot analyses of nonconcentrated supernatants and membrane fractions, respectively. wt, wild-type FhaC; ΔL6, FhaC lacking loop L6. (B) Electrophysiological behavior of the FhaC derivative lacking L6. The current-voltage curve is shown, with the arrows indicating the direction of the applied voltage ramp. This *I-V* curve should be compared to that of wild-type FhaC reported in Méli *et al*. (*16*). (C) Single-channel recordings at +30 and +50 mV. The dashed lines represent the zero current level. C and O represent the closed and opened states of one channel, respectively. (D) Amplitude histogram of the single-channel recordings at +30mV, illustrating the distribution of the current values between the closed (C) and opened (O) states of one channel. The main conductance of this channel is equal to 0.6 nS. (**E** and **F**) Behavior of FhaC-ΔPOT1 and FhaC-ΔPOT2. (E) Secretion of Fha44 by UT5600 (pFJD12, pFc33) (left lanes), UT5600 (pFJD12, pAS-FcΔPot1) (middle lanes), and UT5600 (pFJD12, pAS-FcΔPot2) (right lanes). Fha44 (top) and FhaC (bottom) were detected with appropriate antibodies by immunoblot analyses of nonconcentrated supernatants and membrane fractions, respectively. wt, ΔP1, and ΔP2 represent wild-type FhaC and FhaC lacking POTRA 1 or POTRA 2, respectively. The positions of the relevant proteins are indicated by arrowheads. The anti-FhaC immunoblot had to be developed for a long period of time, most likely because the deletion variants were poorly recognized by the antibodies and their levels of production were lower than that of the wild-type protein. (F) Electrophysiological behavior of FhaC-ΔPOT1 and FhaC-ΔPOT2. Current-voltage (*I-V*) curves are shown for the two proteins. These *I-V* curves should be compared to that of wild-type FhaC reported in Méli *et al*. (*16*). The arrows indicate the direction of the applied voltage ramp. Note that the I-V curve of FhaC-ΔPOT1 is similar to that of the wild-type protein, unlike that of FhaC-ΔPOT2, in keeping with the respective positions of the two domains relative to the barrel.

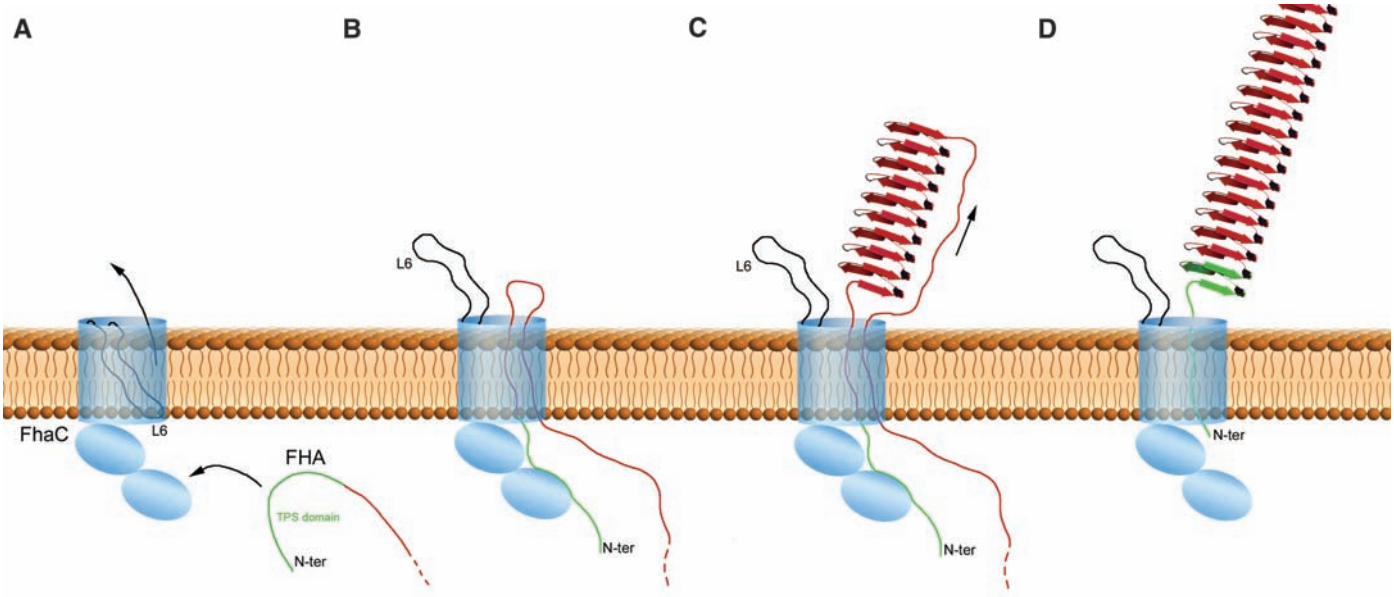

Fig. 4. Proposed model of FHA transport across the outer membrane. (**A**) The TPS domain of FHA in an extended conformation interacts with POTRA 1 of FhaC. (**B**) The channel opens after conformational changes of loop L6, and translocation initiates, with FHA adopting transiently an extended β hairpin structure. (**C**) FHA progressively folds and elongates into its β-helical fold. (**D**) After the C terminus of FHA has reached the surface, the TPS domain dissociates from POTRA 1 and is translocated. The folding of the TPS domain caps the N terminus of the FHA β helix.

gle and double substitutions were created in each of these secondary structures, and the ability of FhaC variants to interact with FHA was assessed (fig. S6) by using an overlay assay developed previously (*25*). Modifications in H2 affected FHA recognition by FhaC in this overlay assay, indicating that helix H2 forms part of the specific recognition surface of FHA.

Collectively, previous data (*15*) and our new mutagenesis data indicate that the L6 loop–motif 3 and the POTRA domains, which are the hallmark features of the superfamily, constitute the active secretion elements of FhaC. FHA is a 50-nm elongated right-handed parallel β helix (*26*–*28*), with the adherence determinants presented on loops or extrahelical motifs along the β helix. The helix interior is essentially filled with stacks of aliphatic residues (Val, Leu, Ile, Ala, and Gly), a characteristic often observed in such β helices. In the light of our structural and functional analysis of FhaC, we propose the following model for transport of FHA across the outer membrane (Fig. 4). The N-terminal TPS domain of FHA, which is characteristic of TpsA proteins and harbors specific secretion signals, initially interacts in an extended conformation with the POTRA 1 domain in the periplasm. Given the orientation of the POTRA domains relative to the channel, the FHA-FhaC interactions bring the region corresponding to the first repeats of the central β-helical domain of FHA in proximity to the tip of loop L6. Conformational changes in FhaC would then expel loop L6 out of the β barrel, opening a 8 Å to 16 Å large (depending on whether H1 is inside or outside the channel during secretion) channel for FHA translocation (fig. S4, C and D). In either case, the channel would not be wide enough to support internal folding of the repeated β-helical motifs of FHA; thus, this event likely takes place at the cell surface. FHA may form a hairpin made up of two extended polypeptide chains in the channel, with its TPS domain anchored in the periplasm. The first repeats of the adhesin could then reach the cell surface, where they could progressively fold into β-helical coils. The formation of the FHA rigid β helix may provide the energy to drive its translocation through FhaC. Transport of FHA in this direction is in agreement with the observation that the C terminus of FHA is exposed to the cell surface before its N terminus (*29*). After the C terminus of FHA has reached the surface, the TPS domain could dissociate from the POTRA domains and be translocated, capping the N terminus of the FHA β helix. Lastly, loop L6 could move back into the barrel.

Because most TpsA proteins are predicted to fold into β helical structures (*26*, *27*), the transport mechanism proposed here may apply more generally to the secretion of TpsA proteins by their dedicated TpsB transporters. All members of the Omp85-TpsB superfamily harbor one to several POTRA domains followed by a β barrel, as well as conserved motifs corresponding to the L6 loop within the barrel, and they mostly handle substrate proteins rich in β structure. Therefore, the major features described here are likely to remain valid throughout the family, although more complex molecular events are expected for some of those transporters, given that they are part of macromolecular assemblies.

References and Notes

1. M.-R. Yen *et al.*, *Biochim. Biophys. Acta* **1562**, 6 (2002).
2. F. Jacob-Dubuisson, R. Fernandez, L. Coutte, *Biochim. Biophys. Acta* **1694**, 235 (2004).
3. S. C. Hinnah, K. Hill, R. Wagner, T. Schlicher, J. Soll, *EMBO J.* **16**, 7351 (1997).
4. B. Bolter, J. Soll, A. Schulz, S. Hinnah, R. Wagner, *Proc. Natl. Acad. Sci. U.S.A.* **95**, 15831 (1998).
5. V. Kozjak *et al.*, *J. Biol. Chem.* **278**, 48520 (2003).
6. S. A. Paschen *et al.*, *Nature* **426**, 862 (2003).
7. R. Voulhoux, M. P. Bos, J. Geursten, M. Mols, J. Tommassen, *Science* **299**, 262 (2003).
8. I. Gentle, K. Gabriel, P. Beech, R. Waller, T. Lithgow, *J. Cell Biol.* **164**, 19 (2004).
9. T. Wu *et al.*, *Cell* **121**, 235 (2005).
10. I. E. Gentle, L. Burri, T. Lithgow, *Mol. Microbiol.* **58**, 1216 (2005).
11. L. Sanchez-Pulido, D. Devos, S. Genevrois, M. Vicente, A. Valencia, *Trends Biochem. Sci.* **28**, 523 (2003).
12. R. Voulhoux, J. Tommassen, *Res. Microbiol.* **155**, 129 (2004).
13. S. Moslavac *et al.*, *FEBS J.* **272**, 1367 (2005).
14. Materials and methods are available as supporting material on *Science* Online.
15. S. Guédin *et al.*, *J. Biol. Chem.* **275**, 30202 (2000).
16. A. C. Méli *et al.*, *J. Biol. Chem.* **281**, 158 (2006).
17. P. Van Gelder, F. Dumas, M. Winterhalter, *Biophys. Chem.* **85**, 153 (2000).
18. The POTRA domains superimpose with an RMS displacement of 1.6 Å, calculated for the Cα. Well-conserved secondary structures include helices H2 and H4, strands β2 and β5, and strands β3 and β6 from POTRA 1 and POTRA 2, respectively.
19. Single-letter abbreviations for the amino acid residues are as follows: A, Ala; C, Cys; D, Asp; E, Glu; F, Phe; G, Gly; H, His; I, Ile; K, Lys; L, Leu; M, Met; N, Asn; P, Pro; Q, Gln; R, Arg; S, Ser; T, Thr; V, Val; W, Trp; and Y, Tyr.
20. C. J. Oomen *et al.*, *EMBO J.* **23**, 1257 (2004).
21. Planar lipid bilayer experiments on the translocator domain of NalP revealed openings and closings of pores of two sizes, with single-channel conductances of 0.15 nS and 1.3 nS that correspond to pore dimensions of 2.4 Å and 8.4 Å, respectively (*20*). Displacement of the α helix from the pore would result in an open channel that may correspond to the observed 1.3-nS conductance steps in planar lipid bilayer experiments. Furthermore, deletion of the α helix in NalP was also shown to increase pore activity (*20*). This helix must be outside the channel to allow for secretion of the passenger domain and could subsequently move in to plug the pore.
22. K. L. Lou *et al.*, *J. Biol. Chem.* **271**, 20669 (1996).
23. N. Saint *et al.*, *J. Biol. Chem.* **271**, 20676 (1996).
24. P. S. Phale *et al.*, *Proc. Natl. Acad. Sci. U.S.A.* **94**, 6741 (1997).
25. H. Hodak *et al.*, *Mol. Microbiol.* **61**, 368 (2006).
26. A. V. Kajava *et al.*, *Mol. Microbiol.* **42**, 279 (2001).
27. B. Clantin *et al.*, *Proc. Natl. Acad. Sci. U.S.A.* **101**, 6194 (2004).
28. FHA comprises an N-terminal TPS domain folded into a β helix, with three extrahelical motifs, a β hairpin, a four-stranded β sheet, and an N-terminal capping (*27*). The reported structure of a 30-kD N-terminal fragment of FHA (Fha30) also reveals several β-helical repeats that form the central right-handed β helix domain of the full-length adhesin.
29. J. Mazar, P. A. Cotter, *Mol. Microbiol.* **62**, 641 (2006).
30. W. L. DeLano, PyMOL Molecular Graphics System (2002); www.pymol.org.

31. We thank H. Hodak for the gift of Fha30 and FhaC-N^{myc} and for advice with the overlay assay experiments, E. Willery and M. L. Parsy for the antibiotic susceptibility experiments, H. Belrhali for support at beamline BM14 at the European Synchrotron Radiation Facility (ESRF, Grenoble), and H. Drobecq for expert assistance with the mass spectrometry experiments. A.C.M. and P.R. are the recipients of predoctoral fellowships from the French Minister de l'Education Nationale and Recherche and Technologie. B.C., F.J.-D., and V.V. are researchers of the CNRS. This work was supported in part by an ACI BCMS2004 grant from the French Ministry of Research. V.V. is supported by an Action Thématique et Incitative sur Programme program from the CNRS and by the Region Nord-Pas de Calais through the Contrat de Plan État-Région and Fonds Européen de Développement Régional programs. Coordinates and structure factors have been deposited in the Protein Data Bank with accession code 2QDZ.

Supporting Online Material

www.sciencemag.org/cgi/content/full/317/5840/957/DC1
Materials and Methods
Figs. S1 to S6
Tables S1 and S2
References

16 April 2007; accepted 11 July 2007
10.1126/science.1143860

Structure and Function of an Essential Component of the Outer Membrane Protein Assembly Machine

Seokhee Kim,[1] Juliana C. Malinverni,[2] Piotr Sliz,[3,4] Thomas J. Silhavy,[2] Stephen C. Harrison,[3,4] Daniel Kahne[1,3]*

Integral β-barrel proteins are found in the outer membranes of mitochondria, chloroplasts, and Gram-negative bacteria. The machine that assembles these proteins contains an integral membrane protein, called YaeT in *Escherichia coli*, which has one or more polypeptide transport–associated (POTRA) domains. The crystal structure of a periplasmic fragment of YaeT reveals the POTRA domain fold and suggests a model for how POTRA domains can bind different peptide sequences, as required for a machine that handles numerous β-barrel protein precursors. Analysis of POTRA domain deletions shows which are essential and provides a view of the spatial organization of this assembly machine.

Although most biological membranes contain exclusively α-helical proteins, the outer membrane of Gram-negative bacteria and the organellar membranes of mitochondria and chloroplasts contain β-barrel proteins (*1*). These integral β-barrel proteins, called outer membrane proteins (OMPs), are folded and inserted into membranes by a process, conserved between prokaryotes and eukaryotes (*2*–*4*), that involves the action of a multiprotein